PERGAMON

Vision Research 40 (2000) 2677–2696

Vision Research

www.elsevier.com/locate/visres

# Performance asymmetries in visual search demonstrate failure of independent-processing models

Barbara Zenger [a,*], Manfred Fahle [b,c]

[a] *Department of Psychology, Stanford University, Stanford, CA 94305-2130, USA*
[b] *Department of Optometry and Visual Science, 311–321 Goswell Road, London EC1V 7DD, UK*
[c] *Center for Cognitive Science, Human Neurobiology, Argonnenstr. 3, D28211 Bremen, Germany*

Received 28 June 1999; received in revised form 12 January 2000

**Abstract**

We report psychophysical data from orientation-popout experiments that are inconsistent with a rather general decision model. Stimuli consisted of 121 line segments arranged on an $11 \times 11$ grid. There were two tasks: in the 1-Singleton Task all lines except one had the same orientation, and observers had to report which quadrant contained the singleton. In the 3-Singleton Task three quadrants contained orientation singletons and observers had to identify the quadrant without singleton. These tasks can be viewed as asymmetric search tasks, in which either a singleton-quadrant has to be found among three homogeneous quadrants, or a homogeneous quadrant has to be found among three singleton-quadrants. Using tools from signal-detection theory we show that the large performance asymmetries between 1-Singleton and 3-Singleton Tasks are inconsistent with any model that makes two (very basic and common) assumptions: (1) independent processing of the four quadrants and (2) an ideal-observer decision. We conclude that at least one of the two assumptions is inadequate. As a plausible reason for the model failure we suggest a global competition between salient elements that reduces popout strength when more than one singleton is present. 

*Keywords:* Human psychophysics; Modeling; Visual search; Performance asymmetry; Signal detection theory

## 1. Introduction

In a visual search task, the observer has to detect a defined target element among distractors. Some search tasks are effortless; for instance, when a red target has to be found among green distractors the target pops out, and search performance is independent of the number of distractors in the display (Treisman & Gelade, 1980). Performance in a specific search task is most commonly assessed by measuring reaction times for target detection (Treisman & Gelade, 1980; Wolfe, 1994). In a related paradigm, stimulus displays are presented only briefly (as short as 5 ms), and processing time is limited by the presentation of a mask, typically a compound of target and distractor items. In this case, performance is described as the minimal time interval between stimulus onset and mask onset (stimulus onset asynchrony, or short, SOA) that allows for correct detection at a defined accuracy level (Bergen & Julesz, 1983; Sagi & Julesz, 1985).

Perhaps the most intensively studied popout task is orientation popout. Here, the background lines all have the same orientation, and only one line segment differs in orientation. It is widely accepted that the detection of the orientation singleton results from a process that operates in parallel over the visual field (Treisman & Gelade, 1980; Nothdurft, 1985, 1991; Bacon & Egeth, 1991; Palmer, Ames & Lindsey, 1993; Ahissar & Hochstein, 1996). When two or three singletons are presented in a display, they all pop out (Sagi & Julesz, 1985; Nothdurft, 1991). Here we report data from popout experiments which are inconsistent with a model that assumes: (1) independent processing of different elements (here: quadrants) and (2) an ideal-observer decision.

* Corresponding author. Tel.: +1-650-725-3046; fax: +1-650-725-5699.

*E-mail addresses:* barbara@white.stanford.edu (B. Zenger), mfahle@uni-bremen.de (M. Fahle).

0042-6989/00/$ - see front matter 
PII: S0042-6989(00)00116-4

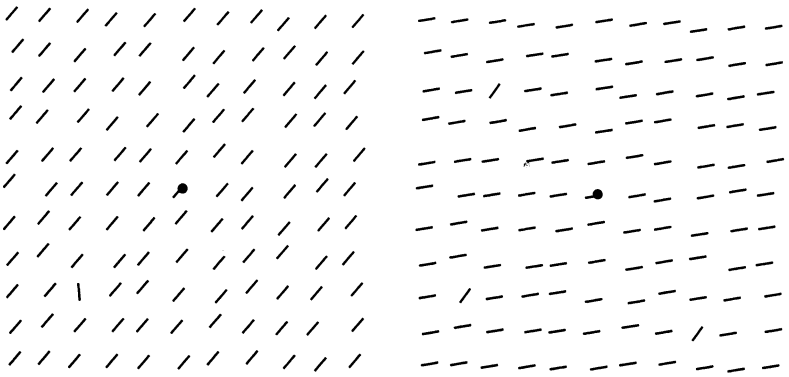

Fig. 1. Examples of stimuli. In the 1-Singleton Task, observers have to find the quadrant that contains the singleton; in the 3-Singleton Task, observers have to locate the quadrant without the singleton. Stimuli were presented for 14 ms. After a blank stimulus (whose duration was varied to adjust task difficulty) a mask was shown, in which each line segment of the stimulus was replaced by two randomly oriented line segments. A fixation point was presented at the display center.

The psychophysical experiment consisted of two different tasks: a 1-Singleton Task and a 3-Singleton Task (see Fig. 1). In the 1-Singleton Task, one of the four quadrants contained an orientation singleton, and observers had to report which quadrant contained the singleton (four-alternative forced choice; 4AFC). In the 3-Singleton Task three quadrants contained a singleton and observers were asked to report which quadrant did not contain a singleton. On a more abstract level one can view these tasks as search tasks with four elements (quadrants). The only difference between the 1-Singleton and 3-Singleton tasks is that the role of target and distractors is reversed (see Fig. 2). Performance differences between such tasks (where target and distractor items are exchanged) are commonly referred to as search asymmetries or performance asymmetries, and have often been observed (Treisman & Souther, 1985; Treisman & Gormican, 1988; Driver & McLeod, 1992; Cohen, 1993; Meigen, Lagreze & Bach, 1994; Nagy & Cone, 1996).

We show that the large performance asymmetries obtained in the 1-Singleton and 3-Singleton Tasks are inconsistent with a very general decision model, which we refer to as Independent-Processing Model (IPM). In this model, no assumptions are made about specific low-level mechanisms, such as feature detection, nonlinear response characteristics, or singleton detection; instead, early processing is simply treated as a black box. For each element (here: quadrant) there exists a black box that receives the stimulus as input and produces a response as its output. These responses are noisy, i.e. for any given stimulus the response is described by a distribution and not a fixed number. We would like to emphasize that we do not require that the black box itself operates in an optimal fashion. We do, however, require that the final decision, based on all the different black box outputs, is ideal. This general model includes several more specific search models. In particular, there are a variety of recent search models (Palmer, Ames & Lindsey, 1993; Palmer, 1994; Eckstein & Whiting, 1996; Laarni, Nasanen, Rovamo & Saarinen, 1996; Zenger & Fahle, 1997; Foley & Schwarz, 1998; Eckstein, 1998; for a review see Palmer, Verghese & Pavel, 2000) that assume Gaussian noise for each element and then pick the maximum response (which is ideal when target-likelihood increases with increasing response).

If the response distributions of singleton quadrants and homogeneous quadrants are known, one can predict performance levels in the 1-Singleton and the 3-Singleton Tasks. As an example, one might assume that the distributions look like the probability density distributions $f_A$ and $f_B$ in Fig. 3. In the 1-Singleton Task, the singleton quadrant usually produces larger responses than the homogeneous quadrants, and, consequently, it is optimal to choose the quadrant with the largest response. The probability of a correct response, thus, equals the probability that a random sample taken from distribution $f_A$ is larger than each of three random samples taken from distribution $f_B$. It can be shown that the two distributions $f_A$ and $f_B$ completely determine the percentage of correct responses (see below for a detailed calculation). In the 3-Singleton Task, the stimulus contains three singleton quadrants and one homogeneous quadrant. Here, the ideal strategy is to

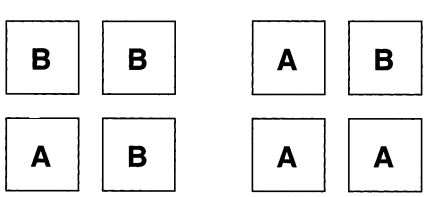


Fig. 2. On a more abstract level the 1-Singleton and 3-Singleton Tasks can be considered as search tasks. In the 1-Singleton Task the singleton quadrant (element A) has to be found among three homogeneous quadrants (elements B). In the 3-Singleton Task a homogeneous quadrant (element B) has to be found among three singleton quadrants (elements A).

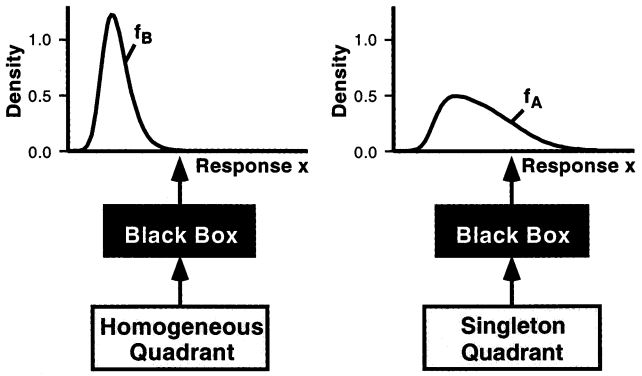


Fig. 3. Example of response distributions for singleton quadrants ($f_A$) and homogeneous quadrants ($f_B$). Probability densities are plotted as a function of response $x$ (in the decision unit). The area under the curve between two response values $x_1$ and $x_2$ indicates the probability that the response in the decision unit is between $x_1$ and $x_2$. Singleton quadrants produce (on average) larger responses than homogeneous quadrants, therefore, the optimal decision strategy is to choose the quadrant with the largest response in the 1-Singleton Task and to choose the quadrant with the smallest response in the 3-Singleton Task.

choose the smallest of the four responses, and the probability of a correct response is, thus, equal to the probability that one random sample taken from distribution $f_B$ is smaller than each of three random samples taken from distribution $f_A$.

Trying to predict performance in the two tasks one faces only one serious problem: nothing is known about the form of the two distributions $f_A$ and $f_B$. It can be shown that it is, nevertheless, possible to derive strong constraints on the magnitude of performance asymmetries. The psychophysical data are not consistent with these constraints because the performance difference between 1-Singleton and 3-Singleton Tasks is larger than the differences predicted by the IPM. Therefore, the model has to be rejected, in spite of its generality.

## 2. Modeling

### 2.1. Basic concepts of signal-detection theory

The rejection of the IPM is based on an analysis using signal-detection theory. Some basic concepts of this theory will briefly be introduced here (see also Green & Swets, 1966).

#### 2.1.1. Density distributions and cumulative distributions

The response distributions of two arbitrary elements (elements A and B) can be represented in *density curves* $f_A$ and $f_B$. Dividing the two density functions $f_A(x)$ and $f_B(x)$ gives the *likelihood ratio*. For the following analysis, we will assume that this likelihood ratio is a monotonic function of $x$, meaning that the likelihood that element A is present (rather than element B) does not decrease with increasing response $x$. This assumption is referred to here as monotonicity assumption. It will be shown below (Section 2.3.1) that this assumption is not critical for the model prediction, but it simplifies the analysis (and the assumption appears reasonable).

Instead of density distributions $f$ it is sometimes convenient to consider the *cumulative distributions* $F$ with

$$F(x_0) = \int_{-\infty}^{x_0} f(x)\mathrm{d}x \qquad f(x) = \frac{\mathrm{d}F(x)}{\mathrm{d}x} \tag{1}$$

A specific point $F(x_0)$ represents the probability that the response produced by the stimulus is less than $x_0$.

#### 2.1.2. The receiver operator characteristic

A further common representation of the statistical distributions of the two elements is the *receiver operator characteristic* (ROC) where the hit rate is plotted against the false-alarm rate. To understand the meaning of the ROC curve, one can imagine an experiment where one of the elements A and B is presented, and the observer has to tell whether or not this element was the (defined) target element. Depending on whether element A or B is defined as the target, different ROC curves are obtained.

Let us first consider the case where element A is the target, and element B is the distractor. To discriminate between the two elements, observers use an internal criterion $c$. When the response is above the criterion, they decide 'target present', when the response is below, they decide 'target absent'. The hit and false-alarm rates corresponding to a specific criterion $c$ are shown as shaded areas in Fig. 4. A 'pessimistic' observer might set the criterion to a high value to reduce false-alarms (of course, this also reduces the hit rate). A more 'optimistic' observer may take low response values already as sufficient evidence for target presence, and set the criterion to a lower response level (causing an increase in both false-alarm and hit rates). For all the different criterion locations $c$, one obtains a specific hit rate (given by $1-F_A(c)$, see Fig. 4) and a specific false-alarm rate (given by $1-F_B(c)$, see Fig. 4). All these different criteria can be represented in a single graph by plotting the hit rate against the false-alarm rate, resulting in the ROC shown in Fig. 5 (panel on the left-hand side).

If element B serves as target (instead of element A) one will decide 'target present' if the response is below the decision criterion. The expected hit and false-alarm rates are represented by the shaded areas in the lower panel of Fig. 4. The corresponding ROC curve (where $F_B$ is plotted against $F_A$) is shown in Fig. 5 (panel on the right-hand side).

Note that the two ROCs correspond to each other as they are both based on the functions $F_A$ and $F_B$. Geometrically, this correspondence is reflected in the

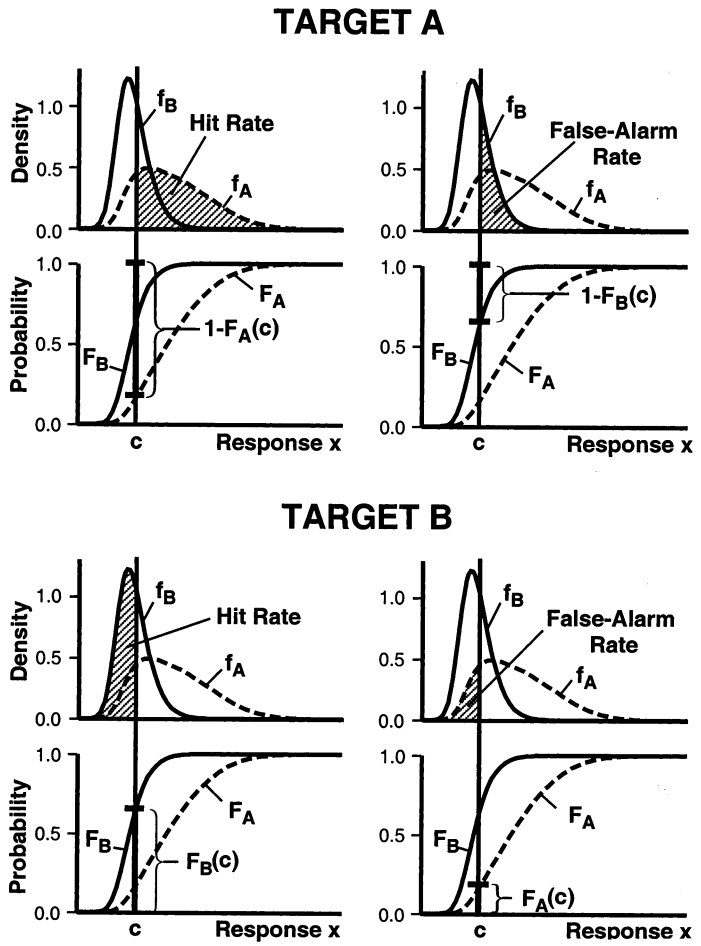


Fig. 4. Hit and false-alarm rates for targets A and B, in a task where in each trial either element A or element B is presented, and observers have to decide whether or not the presented element was the target. Hit and false-alarm rates (represented by shaded areas under the density curves) depend on the internal decision criterion $c$ (solid vertical line) that is used by the observer. Each of these shaded areas corresponds to the length of the line segment either above or below the intersection of the cumulative distributions ($F_A$ or $F_B$) with the criterion $c$, as indicated in the lower diagrams in both panels. The corresponding ROC curves (see Fig. 5) are obtained by plotting the hit rate against the false-alarm rate for all possible criterion locations $c$.

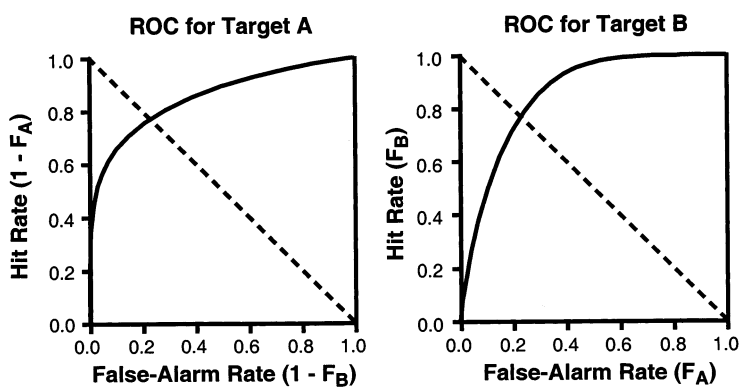


Fig. 5. ROCs for element A as target and element B as target. Both curves depend on $F_A$ and $F_B$. The correspondence between the two curves is reflected in the fact that they are mirror symmetric to each other with respect to the diagonal (dashed lines). The area under the ROC curves corresponds to the performance in a 2AFC task.

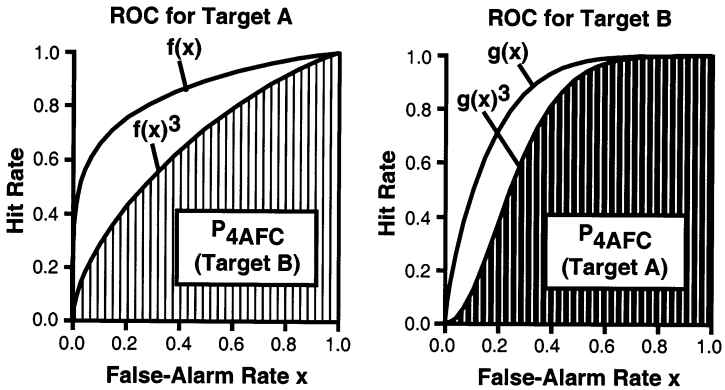


Fig. 6. Taking the ROCs for targets A and B to the power of three and then integrating gives performance in the 4AFC for targets B and A.

fact that the two curves can be transformed onto each other by a mirror reflection on the diagonal ($y = 1 - x$; dashed lines in Fig. 5). Knowing the ROC for target element A is, thus, sufficient for determining the ROC for target element B, and vice versa.

### 2.1.3. Properties of the ROC curve

One important property of the ROG is that its slope can be interpreted as the likelihood ratio between target and distractor (Green & Swets, 1966). The slope in the ROC for target element B, e.g. is given by

$$m_{\mathrm{ROC}} = \frac{F_{\mathrm{B}}(c_1) - F_{\mathrm{B}}(c_0)}{F_{\mathrm{A}}(c_1) - F_{\mathrm{A}}(c_0)} \cdot \frac{1/(c_1 - c_0)}{1/(c_1 - c_0)} \underset{c_1 \to c_0}{=} \frac{F'_{\mathrm{B}}(c_0)}{F'_{\mathrm{A}}(c_0)} = \frac{f_{\mathrm{B}}(c_0)}{f_{\mathrm{A}}(c_0)} \tag{2}$$

(Green & Swets, 1966). An implication of this property is that ROC curves have a monotonically decreasing slope: when element A is the target, for instance, an increase in the false-alarm rate is obtained by a leftward shift of the decision criterion. This shift corresponds to a decrease in target likelihood (this is where the monotonicity assumption comes in), and, thus, corresponds to a decrease in the slope of the ROC curve. This means that the slope of the ROC decreases for increasing false-alarm rate (abscissa of the ROC) and implies that the ROC curve is convex. The required convexity of ROCs plays an important role in the derivation of the IPM predictions.

### 2.1.4. Computing the probability of a correct response in 2AFC and 4AFC experiments

A useful property of the ROC is that the area under the curve is equal to the performance level in a 2AFC where elements A and B have to be discriminated (Green & Swets, 1966). To understand this property, let us again first consider the case where element A is the target: assuming that the target produces a response of $x_0$, the decision will be correct when the response of the distractor (element B) is below $x_0$, and this occurs with a probability of $F_{\mathrm{B}}(x_0)$. Integrating over all possible $x_0$ values (weighted with the probability that element A produces this specific response), we obtain for the performance in a 2AFC with target element A (Green & Swets, 1966):

$$\begin{aligned} P_{\mathrm{2AFC}} &= \int_{-\infty}^{\infty} F_{\mathrm{B}}(x_0) \cdot f_{\mathrm{A}}(x_0)\mathrm{d}x_0 \\ &= \int_{-\infty}^{\infty} F_{\mathrm{B}}(x_0) \cdot \frac{\mathrm{d}F_{\mathrm{A}}(x_0)}{\mathrm{d}x_0}\,\mathrm{d}x_0 \\ &= \int_0^1 F_{\mathrm{B}}(F_{\mathrm{A}})\mathrm{d}F_{\mathrm{A}} \end{aligned} \tag{3}$$

Note that $F_{\mathrm{B}}(F_{\mathrm{A}})$ is the mathematical description of the ROC curve for target element B (see Fig. 5). The probability of a correct response can, thus, be interpreted as the area under the ROC for target element B. In the 4AFC task where element A has to be found among three elements B, the responses of all three distractors have to be below the target response $x_0$, and this happens with a probability of $F_{\mathrm{B}}(x_0)^3$. For the probability of a correct response in a 4AFC, we thus obtain

$$P_{\mathrm{4AFC;Target\ A}} = \int_0^1 F_{\mathrm{B}}(F_{\mathrm{A}})^3\,\mathrm{d}F_{\mathrm{A}} \tag{4}$$

(Green & Swets, 1966). The performance can again be visualized geometrically (Green & Swets, 1966): if one takes the ROC for target element B to the power of three, the performance level corresponds to the area under the resulting curve (see dark shaded area in Fig. 6). Note that there is a peculiar switch in target roles: although we have considered the case where *element A* is the target in the AFC tasks, we obtain the corresponding performance by integrating over the ROC curves for target *element B*.

An analogous derivation can be made for the case in which element B (rather than element A) is the target. One finds that performance in the 2AFC corresponds to the area under the ROC curve for target element A.

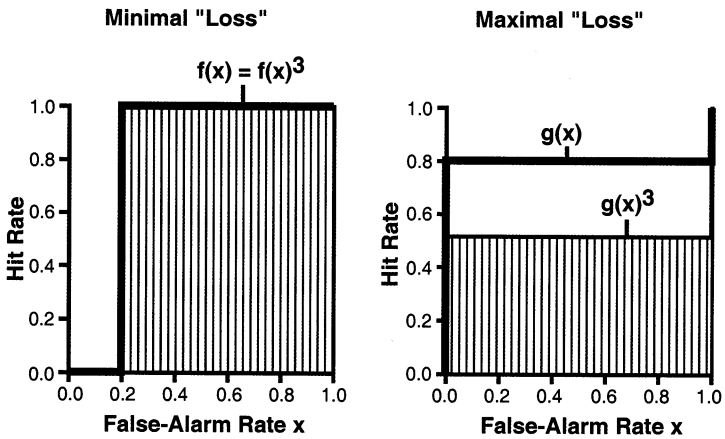


Fig. 7. ROC curves that maximize and minimize performance in a 4AFC task for a given performance level of 80% in the 2AFC task. The solutions, are, however, inconsistent with the monotonicity assumption because the ROC curves are not convex.

Performance in the 4AFC (where element B has to be found among three elements A) is obtained by taking this ROC to the power of three and then integrating (see lightly shaded area in Fig. 6).

In a 2AFC, it does, of course, not really matter for the task which of the two elements is defined as target. This equivalence is reflected by the fact that the area under the ROC does not change as a result of the mirror reflection along the diagonal (dashed lines in Fig. 5). In the 4AFC, however, it *does* matter which of the two elements serves as target and which serves as distractor. Because of the power manipulation, the dark and light shaded areas in Fig. 6 (which correspond to the two performance levels) are not necessarily equivalent. The difference between them reflects a performance asymmetry.

In summary, two concepts are of particular importance:

- The statistical response distributions of elements A and B can be represented in two convex ROC curves which are mirror symmetric to each other with respect to the diagonal.
- Performance in the two asymmetric 4AFC tasks is obtained by taking these ROCs to the power of three and then integrating.

### *2.2. Estimating an upper limit for performance asymmetries*

The two ROC curves cannot be modified independently (they have to be mirror symmetric with respect to the diagonal). Therefore, one expects that the performance levels in the two 4AFC tasks depend on each other.

To give a simple example: assume that performance in a specific 2AFC task is 100% — what performance level is expected in the corresponding 4AFC tasks? It is easy to see that the performance level of 100% in the 2AFC implies that the ROC covers the whole area. Thus, the ROC is described as $y = 1$. This curve does not change when taken to the power of three. Therefore, one can conclude that performance in the 4AFC will also be perfect. This is, of course, a trivial example; no particularly surprising insight is obtained here.

Assume now that one knows that performance in the 2AFC is 80%. Can anything be said about the expected performance level in the corresponding 4AFC tasks? What we would ideally like to have is a statement like: if the percentage of correct responses in a 2AFC is 80%, the percentage of correct responses in the corresponding 4AFCs should be at least $X_{\min}$, but not more than $X_{\max}$. The question can be rephrased as the following task: construct a ROC that covers 80% of the area, and that 'loses' as little (or as much) area as possible when taken to the power of three.

Starting with the idea of minimal area loss: there is no loss if the ROC assumes only the values '0' and '1'. The optimal curve could, thus, look like the one shown in Fig. 7 (left-hand side). This curve covers an area of 80%, and it does not change when taken to the power of three. However, the proposed curve is not a reasonable ROC because, as mentioned before, ROCs have to be convex. With this additional constraint, the optimal ROC is the one shown in Fig. 8 (left-hand side). Similarly, if the loss of area is to be maximized, one can show that, in the optimal case, all values of the ROC are equivalent. Assuming again that the curve should cover 80% of the area, one will, consequently, come up with the curve shown in Fig. 7 (right-hand side). Unfortunately, this curve is again not convex; if convexity is taken into account, the optimal curve looks like the one shown in Fig. 8 (right-hand side). A formal proof showing that the proposed curves (see Fig. 8) are indeed optimal in the sense that they produce upper and lower bounds for the performance in a 4AFC

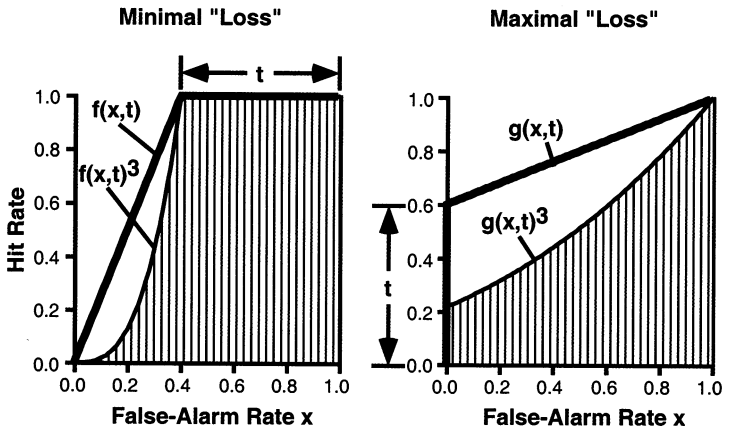


Fig. 8. ROC curves that maximize and minimize performance in a 4AFC task for a given performance level of 80% in the 2AFC task when convexity of the ROC curves is required.

(given a specific performance in the 2AFC) is outlined in Appendix A.

Interestingly, the two graphs in Fig. 8 are mirror symmetric to each other with respect to the diagonal. This means that the ROC that maximizes performance in one of the two 4AFC tasks at the same time minimizes performance in the asymmetric 4AFC task. The two ROCs, thus, represent response distributions that produce the maximal possible performance asymmetry. The shape of these ROCs is, of course, general and not specific to the assumption of 80% correct responses in the corresponding 2AFC. The general curve is easily described by using $t$ for the parameterization of the ROC ($t = 2 \cdot P_{2\mathrm{AFC}} - 1$; see Fig. 8 for a geometrical interpretation of $t$).

The ROC $f(x,t)$ in Fig. 8 is described by

$$f(x,t) = \begin{cases} x/(1-t) & x < 1-t \\ 1 & x \geq 1-t \end{cases} \quad (5)$$

and the ROC $g(x,t)$ in Fig. 8 is described by

$$g(x,t) = t + (1-t)x \quad (6)$$

Taking these functions to the power of three and then integrating, we obtain for the performance in the 'easy' task

$$P_{\mathrm{easy}} = \int_0^1 f(x,t)^3 \mathrm{d}x = \frac{1}{4}(3t+1) \quad (7)$$

For the performance in the 'difficult' task, solving the integral yields

$$P_{\mathrm{difficult}} = \int_0^1 g(x,t)^3 \mathrm{d}x = \frac{1}{4}(t^3 + t^2 + t + 1) \quad (8)$$

Solving Eq. (7) for $t$ we obtain $t = (4 \cdot P_{\mathrm{easy}} - 1)/3$. Inserting this into Eq. (8) and simplifying gives

$$P_{\mathrm{difficult}} = \frac{1}{27}(16 \cdot P_{\mathrm{easy}}^3 + 6 \cdot P_{\mathrm{easy}} + 5) \quad (9)$$

The relationship between the two performance levels is illustrated graphically in Fig. 9, with the shaded area representing asymmetries that are consistent with the IPM.

### 2.3. Model generalizations

#### 2.3.1. Relaxing the monotonicity assumption

When deriving the upper limit for performance asymmetries, we assumed that the target likelihood is a monotonic function of the response $x$ (Section 2.1.1).

We further assumed that observers select the quadrant with the largest response when searching for element A, and that they select the quadrant with the smallest response when searching for element B. It turns out that the monotonicity assumption is not required anymore, when we replace this maximal-or-minimal-response strategy by an ideal-observer decision.

The ideal strategy in a forced choice is to choose the quadrant with the maximal target likelihood (which is

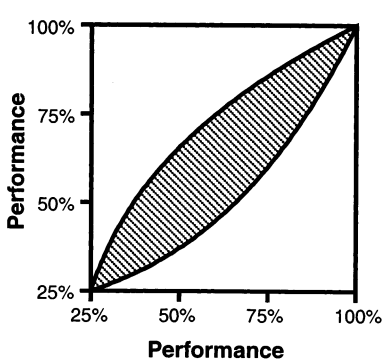


Fig. 9. The two axes represent the performance levels in the two asymmetric 4AFC tasks. The maximal performance asymmetries described by Eq. (9) are shown as solid lines. Combinations of performance levels in the two asymmetric tasks that correspond to points outside the shaded area are inconsistent with the IPM.

Table 1
Evaluation of the probabilities of a correct response in the 1-Singleton and 3-Singleton Tasks, when a singleton is detected with a probability of $P$ (see text for details)

| | Detected singletons | Detection probability $P$ | Guessing probability $p$ | $P \times G$ |
|---|---|---|---|---|
| 1-Sgl task | 1 | $P$ | 1 | $P$ |
| | 0 | $1-p$ | 1/4 | $-1/4p+1/4$ |
| Σ | | | | $3/4p+1/4$ |
| 3-Sgl task | 3 | $p^3$ | 1 | $p^3$ |
| | 2 | $3p^2(1-p)$ | 1/2 | $-3/2p^3+3/2p^2$ |
| | 1 | $3p(1-p)^2$ | 1/3 | $p^3-2p^2+p$ |
| | 0 | $(1-p)^3$ | 1/4 | $-1/4p^3+3/4p^2-3/4p+1/4$ |
| Σ | | | | $1/4p^3+1/4p^2+1/4p+1/4$ |

not necessarily the quadrant that produces the maximal or minimal response). Assuming that human observers are able to make an ideal-observer decision, implies that they are able to select, among several responses, the one that corresponds to the maximal target likelihood. In other words, they behave as if they could map response values $x$ onto likelihood values $l$. One can, thus, define the $l$ values as the new 'response' on which decision is based. For this new response, the monotonicity assumption holds per definition (because likelihood is, of course, a monotonic function of likelihood). The case of arbitrary response distributions is, thus, equivalent to the case of distributions that follow the monotonicity assumption, at least, if we assume that observers are able to make the optimal decision.

### 2.3.2. More than one decision variable per quadrant

What happens if the observer has access to more than one decision variable per quadrant? The observer might, e.g. rely on more than only one discontinuity detector, and, in addition, first-stage units might also have some weight in the decision. Interestingly, if we assume an ideal-observer decision, this general situation is again covered by the IPM. The critical point is that, in principle, all these decision variables can be used to compute a single value, that of target likelihood. It seems questionable whether observers are always able to do such a computation, but assuming an ideal-observer decision implies that observers always choose the quadrant with maximal target likelihood, i.e. they behave as if they could indeed map the multidimensional decision variable onto target-likelihood values.

## 2.4. Equivalence to high-threshold model

A noteworthy observation is that Eqs. (7) and (8), derived for the upper and lower bounds of performance in a 4AFC, are formally equivalent to the performance predictions of a high-threshold model.

The high-threshold model is based on the assumption that the threshold is so high that only a 'real' signal can reach threshold whereas noise alone can never reach the threshold, and, thus, there are no false alarms (Green & Swets, 1966). In other words, the salient element (the singleton quadrant) reaches detection threshold with a certain probability $p$, whereas the non-salient element (the homogeneous quadrant) cannot be detected. This simple assumption of a fixed detection probability allows for a straightforward prediction of the expected performance levels.

The respective calculations are shown in Table 1. The first column gives the number of detected singletons. The second column gives the probability that exactly this number of singletons is detected, and the third column contains the probability of a correct answer, given that exactly this number of singletons is detected. In the 1-Singleton Task, one either detects the singleton — and this occurs with a probability of $p$ — or one does not detect it, and this occurs with a probability of $(1-p)$. In the first case, one always answers correctly, in the second case one has to rely entirely on guessing, and is correct only in one out of four cases. The expected performance is obtained by multiplying the terms in the second and the third column, and summing up across the two rows:

$$P_{\text{1-Sgl}} = \frac{1}{4}(3P+1) \tag{10}$$

In the 3-Singleton Task, the calculation is slightly more complicated, but the idea is the same: one detects either all three singletons, two of them, one of them, or none at all. The corresponding probabilities (second column) are computed according to the binomial distribution. The third column again contains the guessing probabilities, e.g. when two singletons are detected, the probability of finding the homogeneous quadrant is one half. Multiplying column two and three and summing up, we obtain:

$$P_{\text{3-Sgl}} = \frac{1}{4}(p^3+p^2+p+1) \tag{11}$$

One can easily verify that Eqs. (10) and (11) are formally equivalent to Eqs. (7) and (8), which were obtained after taking the ROC curves in Eqs. (5) and

(6) to the power of three and then integrating. This shows that the high-threshold model is equivalent to the maximal-asymmetry condition in the IPM.

The equivalence can become more plausible if we look again at the ROC curves in Fig. 8. The two linear portions of the ROC can be viewed as two separate response categories: The response of an element either allows us to classify it as element A because the likelihood of element B is zero (and, in this situation, the high-threshold model would state 'element reached threshold'), or the response is such that we cannot make a clear classification (reflecting the case where the 'element did not reach threshold').

The equivalence of the two models seems still surprising because they are based on completely different assumptions: in the high-threshold model, we make the rather specific assumptions of a fixed detection probability for a singleton, whereas, in the IPM, the assumptions are much more general: processing in each quadrant is represented by a black box that can produce gradual responses described by statistical distributions (and not just two discrete responses such as 'detected' and 'not-detected'). Yet, if another constraint — the constraint of maximal performance asymmetry — is added to the IPM, one ends up with the same model.

## 3. Methods

Stimulus presentation and data collection were controlled by a Silicon-Graphics work station (Indigo 2). Stimuli were presented on a 19 in. Mitsubishi Raster Monitor with a frame rate of 72 Hz and a resolution of $1280 \times 1024$ pixels. When tilted lines are presented on a raster monitor, the line segments often have a clearly visible zig–zag appearance (as a result of sampling). To minimize this problem, the stimuli were anti-aliased (Bach, 1991). Bright stimuli with a luminance of approximately 90 cd/m$^2$ were presented on a dark background. The room was dimly-lit to facilitate accommodation. Stimuli were viewed from a distance of 60 cm and head position was stabilized by a chin rest.

Stimuli were textures of $11 \times 11$ line segments. Each line segment had a length of $30'$ and a width of $1.5'$. Elements were located in the center ($\pm 10'$ random jitter) of the boxes formed by an imaginary grid, with a box width and height of 1°. Most of the lines had an orientation $\theta_{bg}$ that was varied randomly from trial to trial. One or three background elements were replaced by singletons that had an orientation of $\theta_{sgl} = \theta_{bg} + \Delta\theta$, with $\Delta\theta = 30°$, 45°, 60°, 75° or 90°, pseudo-randomly varied within each block. The location of the singletons was restricted to the second and third columns and rows from the texture edges (see Fig. 1 for examples of the stimuli). In the mask, each line segment of the stimulus was replaced by two randomly oriented line segments at the same location, i.e. the jitter was not changed.

The following asymmetric tasks were designed: a 1-Singleton Task where one orientation singleton is present and observers have to report which quadrant contains the singleton, and a 3-Singleton Task where three quadrants contain a singleton, and observers have to identify the quadrant without singleton (see Fig. 1). Both tasks, thus, have a spatial 4AFC design, and they are asymmetric to each other because the roles of target and distractor are reversed (see Fig. 2). The tasks were performed in separate blocks of 55 trials each (five test trials in the beginning and ten trials for each orientation difference).

A fixation point (with a diameter of $15'$) was visible throughout the experiment. Observers initiated each trial by pressing the space bar. After a 500 ms blank stimulus, stimuli were presented for 14 ms and then replaced by a blank stimulus. Then, a mask was presented for 14 ms and again replaced by a blank stimulus. The time delay between stimulus onset and mask onset (SOA) was varied between different blocks, allowing to adjust task difficulty. Observers responded by pressing specified keys that were arranged on the keyboard corresponding to the four quadrants. A keyboard bell provided feedback following errors.

Since strong learning effects are commonly observed in these types of experiments during the first two sessions (Karni & Sagi, 1991; Ahissar & Hochstein, 1993), each observer participated in at least two practice sessions prior to data collection. In the practice sessions, observers started at a large SOA of 500 ms (or more) and were instructed to perform alternating blocks of the 1-Singleton Task and the 3-Singleton Task until an average performance (averaged across all orientation differences) of at least 60% was reached in both tasks, and, then, to advance to the next SOA level (250, 166, 139, 125 ms, and so on, in steps of 14 ms). The level of 60% ensured that observers were able to solve the task well above chance (25%) and, thus, had a fair amount of practice in both tasks. The actual data were collected within a single session for which SOA was kept constant (varying between 69 and 166 ms for different observers).

Five observers with normal or corrected-to-normal vision participated in the experiment. They were unaware of the purpose of the experiment.

## 4. Results

The results averaged across all five observers are shown in Fig. 10. Accuracies in the 1-Singleton and 3-Singleton Tasks are plotted as a function of the

orientation difference ($\Delta\theta$) between singleton and background. As one would expect, accuracies were in general higher for larger orientation differences.

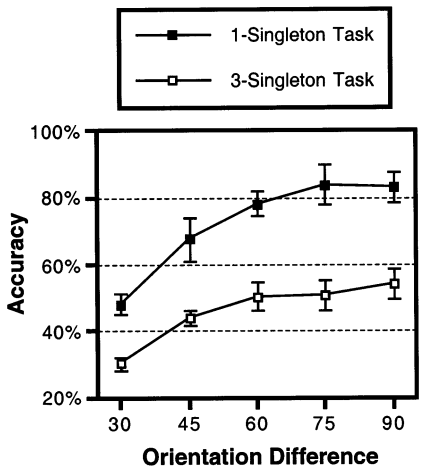


Fig. 10. Performance as a function of the orientation difference between singleton and background elements. The performance difference between 1-Singleton and 3-Singleton Tasks is rather large. Error bars reflect the standard error of the mean across observers.

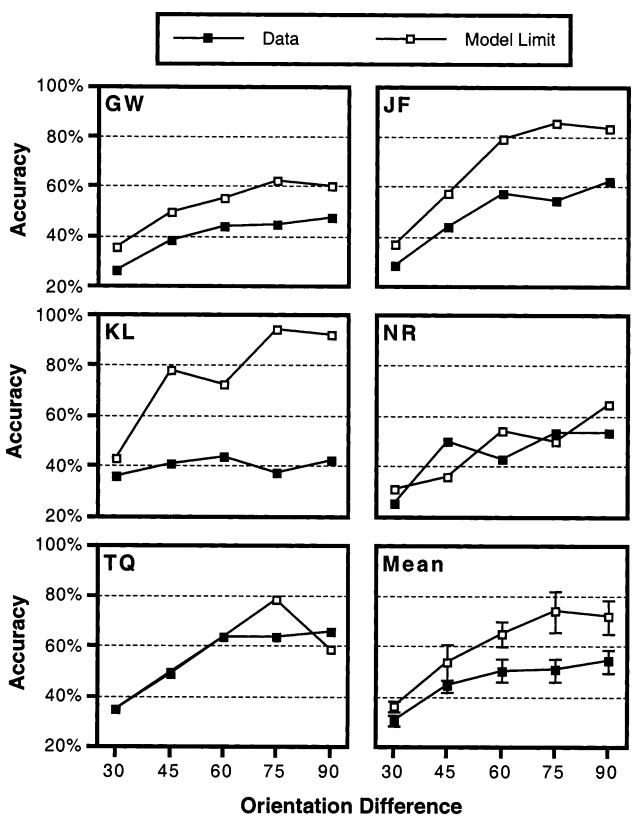


Fig. 11. A lower limit for performance in the 3-Singleton Task was computed based on the performance in the 1-Singleton Task. On average, the actual performance is below the lower limit given by the IPM (error bars reflect the standard error of the mean across observers). The model, thus, has to be rejected.

To test whether the IPM can account for the performance asymmetries, performance in the 1-Singleton Task was entered into Eq. (9) to compute a lower limit for performance in the 3-Singleton Task. These lower limits are presented together with the 'real' performance in the 3-Singleton Task in Fig. 11.

For all observers, the average performance in the 3-Singleton Task is below the lower limit computed by the model (although in two cases the deviations are, by themselves, not convincing). On average, performance in the 3-Singleton Task is consistently below the lower limit defined by the IPM. Therefore, the IPM has to be rejected.

We would like to emphasize that all the observers in this experiment had sufficient practice (two sessions) to be familiar with the task and to optimize their decision strategies; furthermore, the performance asymmetries of the author (BZ, data not shown) remained very consistently above the model limit ($P < 0.001$), even after extensive training. We are thus confident that the failure of the IPM cannot be attributed to a lack of training.

## 5. Discussion

### 5.1. Summary of results

We compared human observers' performance in two tasks: in the 1-Singleton Task the display contained one orientation singleton and observers had to indicate which of the four quadrants contained the singleton. In the 3-Singleton Task three of the four quadrants contained an orientation singleton and observers had to indicate which quadrant contained no singleton. On a more abstract level these two tasks can be viewed as asymmetric search tasks. In one task element A has to be found among three elements B; in the other task element B has to be found among three elements A.

The behavior of a very general decision model, referred to as independent processing model (IPM), was analyzed with tools from signal-detection theory. The model assumes that processing is independent in the four quadrants, and that processing in each quadrant can be described by a black box which receives the stimulus as input and produces a response as output (which can be described in a statistical distribution). The model further assumes an ideal observer decision, i.e. observers select the quadrant with the highest target likelihood (based on the four black-box outputs). This decision strategy is particularly simple when the monotonicity assumption holds, i.e. when the likelihood that element A is present (rather than element B) increases with increasing response (or does at least not decrease). In that case, observers choose either the quadrant with the maximal response (when searching for element A) or the quadrant with the minimal re-

sponse (when searching for element B). The model predicts an upper limit for performance asymmetries that was found to be inconsistent with data from our popout experiments. The IPM is, thus, rejected. The failure of the IPM implies that either the ideal observer assumption or the independent-processing assumption were incorrect.

It was further shown that adding to the IPM the constraint of maximal performance asymmetries leads to a model that is equivalent to a simple high threshold model.

### 5.2. Violations of the ideal-observer assumption

#### 5.2.1. Perceptual bias

It is possible that the response distribution of a specific stimulus is not a fixed distribution, but that it depends on the quadrant in which the stimulus is presented. Such differences between the quadrants could be interpreted as perceptual bias. To test whether perceptual-bias effects can account for the large performance asymmetries found in the experimental data we have extended the IPM to allow for perceptual bias (see Appendix B). Although strong perceptual bias can increase the performance asymmetries, the increase is rather small, and it cannot explain the data. Perceptual bias does, therefore, not appear to be the reason for the failure of the IPM.

#### 5.2.2. Suboptimal decision variables

The IPM assumes an ideal-observer decision. This assumption is convenient for modeling purposes, but one may wonder whether observers are indeed able to estimate the target likelihood of an element based on the activities of all accessible units. In the experiments here, for example, all the units tuned to the different possible singleton locations within the quadrant are expected to contain information about singleton presence or absence. The observer may ignore some units because they contain too little information; memory limitations may come into play, and finally, the observer may be uncertain about which channels contain the signal and may, in addition, monitor some irrelevant channels (Pelli, 1985).

We want to consider this possibility in more detail, using a simple example: assume that the observer monitors two channels (i.e. two independent decision variables) in each quadrant. In the singleton quadrants, one of the two channels contains the singleton signal, the other contains the background signal. In the homogeneous quadrants, both channels contain background signals. Let us further assume that the observer uses the following decision rule: in the 1-Singleton Task, find the maximum response among all eight channels and pick the quadrant that corresponds to this channel; in the 3-Singleton Task, find the minimum response among all eight channels and pick the quadrant that corresponds to this channel. To show that this model can indeed produce large asymmetries let us consider the case where the singleton is highly salient, i.e. singleton responses are always larger than background responses (the distributions show no overlap). In this case, the channel with the maximum response in the 1-Singleton task will always correspond to the singelton quadrant; performance is 100% correct. In the 3-Singleton Task the observer searches for the minimal response. The minimal response occurs with equal chance in any of the five channels that look at background signals. Two of these channel correspond to the homogeneous quadrant (the target), three of these channels belong to the three singleton quadrants (the distractors), the observer thus will find the correct quadrant with a chance of only 40%. Clearly, this model can produce rather large performance asymmetries! However, we would like to argue that the real reason for the large asymmetry does not result from the fact that observers are uncertain about which of the two channels in each quadrant contains the target, but that it results from an unreasonably bad decision strategy.

Let us rephrase the adopted decision strategy slightly: in the 1-Singleton Task the observer first computes the local maximum response (within each quadrant) and then picks the maximum of these responses. In the 3-Singleton the observer first computes the local minimum response (within each quadrant) and then picks the minimum of these four responses. The suggestion that local extrema are computed makes sense; after all, if just one global extremum is estimated the observer may have trouble knowing to which quadrant this extremum corresponds.

Large asymmetries would seem avoidable if the observer uses a better decision strategy. Specifically we suggest that since the observer seems to be able to compute local maxima within each quadrant (the strategy used in the 1-Singleton Task), he or she should be able to apply the same strategy also to the 3-Singleton Task, i.e. the observer should be able to first compute the local maximum in each quadrant, and then pick the global minimum of these local maxima. This is similar to saying that we ask the observer to search for the three singletons, and to infer where the homogeneous quadrant is, rather than to search for homogeneity itself. Using this global-minimum-of-local-maxima strategy observers would reach in the above example a performance level of 100% correct in the 3-Singleton Task, a result that is again consistent with the IPM.

In general, the IPM covers all situations (including uncertainty) where the observer uses the same local strategy for finding the three singletons in the 3-Singleton Task that he or she uses for finding the singleton in the 1-Singleton Task; in other words, the IPM requires that the observer uses the same decision variable in

both tasks. Whether the strategy that is used to find the singleton is ideal, reasonable, or unreasonable is basically irrelevant. If observers use, for instance, the above mentioned global-minimum-of-local-minima strategy for the 3-Singleton Task combined with a global-maximum-of-local-minima strategy for the 1-Singleton Task, predicted performance is poor, but lies within the limits of the IPM.

In short, processes of forgetting and uncertainty reflect suboptimal decisions, but these suboptimal decisions can simply be treated as if they were part of the black box, and thus they cannot account for the large performance asymmetries found in the experimental data. If we exclude the possibility that observers sometimes deliberately choose a quadrant that presumably contains a distractor, the ideal-observer decision does not appear to be a problematic assumption.

### 5.3. Violations of the independent-processing assumption

Independence was assumed because of the large distance between the elements (distance between different singletons was at least 6°). Nevertheless, the assumption may be inadequate.

One possibility is that there are cooperative effects. If two singletons are seen, they could be used to construct an internal square (with the singletons as corners), and this may give observers some indication where in the other two quadrants the third singleton might be found. Another plausible scenario is that there is a response correlation between the quadrants. There may be trials where observers are more sensitive to singletons, and other trials where they are less sensitive. In that case, if observers detect a singleton in one quadrant, they have a higher chance to detect the singletons in the other two quadrants. Such cooperative interactions, however, would suggest that performance in the 3-Singleton Task should be *better* than predicted by the independent-processing assumption. The failure of the IPM indicates that the three singletons apparently do not mutually enhance each others detection, but rather impair it. The interactions between the salient elements thus seem to be of competitive rather than cooperative nature. While such competitive interactions seem quite plausible (Desimone & Duncan, 1995) one can at this point only speculate about possible mechanisms.

#### 5.3.1. Global response normalization

One possibility is that the salience signal of the individual elements is normalized by the sum of the salience signals within the stimulus. Such normalization may be desirable to extract only the most salient elements within a given stimulus. The global-normalization concept strongly reminds of the original account for performance asymmetries given by Treisman and colleagues (Treisman & Souther, 1985; Treisman & Gormican, 1988; see also Gurnsey & Browse, 1989). These authors assume that all responses within the maps are pooled, and that decision is based on this pooled response. They further assume that discrimination of pooled response values follows the Weber Law. Note, however, that the feature-integration model is essentially a first-stage model where feature content is pooled. To account for the data presented here, these first-stage feature maps would have to be replaced by second-stage feature-gradient maps.

#### 5.3.2. Allocation of processing resources

Possibly, the salient signals compete for processing resources. Signals produced by a spatial discontinuity might allocate (in some way) further resources to the respective region, leading to improved singleton detectability. The 3-Singleton Task would then have a disadvantage because the limited resources need to be shared. Note that the additional resources would not only lead to an increase in response, but would also have to decrease the noise level: if large signals simply increase further (due to successful competition), 'false positives' would increase as well as real signals, and discrimination would not improve.

Concepts of resource limitations and processing bottlenecks have often been equated with attentional limitations. Because different authors sometimes have quite different concepts of what exactly is meant when a process is called 'attentional' (Broadbent, 1958; Schneider & Shiffrin, 1977; Posner, 1980; Treisman & Gelade, 1980), it is a difficult task to characterize a specific process as non-attentional. We wish to point out, however, that the resource limitations apparent in our results are different from attentional limitations as they were observed by Braun and colleagues in double-task paradigms (Braun & Sagi, 1990; Braun, 1994; Lee, Koch & Braun, 1997; Braun & Julesz, 1998). In these experiments, attention was taken away from a peripheral task by means of a concurrently performed central task which requires attention. It was found that popout of an orientation singleton is not affected by the concurrent performance in the central task (Braun & Sagi, 1990; Braun, 1994). In other words, concurrent task and additional singletons draw on different resources: singleton processing does not deteriorate in the presence of a concurrent central task that engages attention, but it does deteriorate in the presence of additional singletons.

While this suggests that the singletons do not compete for attention, attention might nevertheless have a strong effect on the global competition. Such effects can be tested in double-task experiments. The concurrent central task does not affect the 1-Singleton Task (Braun & Sagi, 1990), therefore, the critical question is how the central task affects the 3-Singleton Task. Although this experiment has not been carried out here, it

does seem quite unlikely that performing a concurrent task will lead to an improvement in the 3-Singleton Task; rather, one might expect a performance decay. Data of Braun (1994) indeed show that performance asymmetries increase in the absence of attention, which implies that attention reduces the effects of global competition (Braun, 1998).

#### 5.3.3. Memory bottleneck

An obvious possibility is that elements compete for the access to short-term memory. Such competition was suggested, e.g. by Müller and Humphreys (1991) who account for the advantage of cued elements in a luminance increment detection task with an advantage in the selection of the element by the short-term memory. To account for the large performance difference between 1-Singleton and 3-Singleton Tasks, one might suggest that observers can remember only the location (i.e. quadrant) of one or two singletons. Such a memory bottleneck would have no effect on performance in the 1-Singleton Task, but it would dramatically reduce performance in the 3-Singleton Task.

Competition for access to short-term memory is an integral part of the attentional engagement theory proposed by Duncan and Humphreys (1989). These authors suggest that the greater the similarity between element and target template is, the greater is the chance that the element gains access to short-term memory (Duncan & Humphreys, 1992). Our results, however, would suggest that access to short-term memory depends, in addition, on salience: in the 3-Singleton Task, the singleton quadrants apparently win the competition although they are less similar to the target template than the homogeneous quadrants.

### 5.4. Experimental-design requirements

It may seem surprising that the inadequacy of the IPM has not been found in previous studies. The main reason for this may be that the IPM analysis relies heavily on the experimental design used here. Even rather small deviations from this design will lead to results that cannot demonstrate the model's inadequacy (which, of course, does not mean that the model is correct). In the following paragraphs, we would like to point out some of the critical properties of the experimental design used here.

#### 5.4.1. AFC design

The forced-choice design allows implementation of a simple maximum likelihood decision strategy. Assumptions about the setting of decision criteria are not required. Sagi and Julesz (1985) have conducted orientation popout experiments where observers had to count up to four singletons. Since counting requires that the observers use some form of decision criterion, there is no obvious or straightforward way in which these results can be compared to the IPM prediction. Nevertheless, it is surprising that the singleton number apparently had strong effects in the experiments carried out here, and hardly any effect in their experiments.

Solomon, Lavie and Morgan (1997) have performed experiments on brightness discrimination. Stimuli had a spatial layout similar to the one used here, i.e. each quadrant contained one stimulus. The task was to decide whether one of the stimuli had a higher or a lower luminance than the other three stimuli. This task requires a rather elaborate decision strategy: target likelihood increases for responses higher than the baseline as well as for responses lower than the baseline, and in addition, the baseline is not well-defined, but has to be estimated from the four stimuli. The authors did not find any evidence for capacity limitations, i.e. their data seem to be consistent with the IPM. It is not unlikely that capacity limitations could be demonstrated if their stimuli would be used in an asymmetric forced-choice design where observers sometimes have to find the brightest stimulus and sometimes have to find the least bright stimulus.

#### 5.4.2. Small set size

With only four decision variables to be remembered, the task seems to be well within the limits of short-term memory (Miller, 1956; Trick & Pylyshyn, 1994; Luck & Vogel, 1997). It seems thus fair to assume that observers are able to solve the 3-Singleton Task by detecting and remembering the position of the three singletons. If the number of elements is further increased, memory limitations are expected to come into play. The rather large performance asymmetries observed by Braun (1994), who used six elements in each display, may have been affected by such limitations.

An additional advantage of the small element number is that it allows for a rather sparse distribution of elements on the display. As a consequence, observers are not required to make a fine-grained localization, which might require attention (Atkinson & Braddick, 1989). Furthermore, it is the large distance between different elements which makes the assumption of independent processing of the elements more justifiable; i.e. lateral-masking or crowding effects need not be assumed. Note that there are presumably masking or crowding effects between neighboring lines in the display, but these within quadrant processes can be treated as part of the black-box processing and do not contradict the independent-processing assumption.

#### 5.4.3. Only two types of elements

At the decision stage, there were only two types of elements ( = quadrants) in the two asymmetric tasks, e.g. quadrants with singletons and quadrants without singletons. This reduces the number of free parameters enormously. In fact, the two distributions are the only

free parameters. Other performance asymmetry studies on texture segmentation have also used a 4AFC design, but have exchanged foreground and background rather than target and distractor (Gurnsey & Browse, 1987; Rubenstein & Sagi, 1990). For instance, one can compare the performance in segmenting a foreground of randomly oriented Xs from a background of randomly oriented Ls with the performance for segmenting a foreground of randomly oriented Ls from a background of randomly oriented Xs. In these two tasks there are four different types of quadrants: X, L, X-in-L, and L-in-X quadrants. Even if one assumes that only the border signals are relevant (Rubenstein & Sagi, 1990), there are still three critical border signals: X–X, X–L, and L–L borders. The large asymmetries obtained in these studies do not provide evidence for the failure of the IPM (in spite of its inadequacy).

#### *5.4.4. Accuracy measurements*

In the experiments conducted here we measured search accuracy, rather than estimating thresholds at which a fixed performance level is obtained. The rationale here is that thresholds can be compared to signal-detection theory models only if specific assumptions are made about the form of the psychometric functions (Palmer et al., 1993; Verghese & Nakayama, 1994), increasing the degrees of freedom for the data fitting.

#### *5.4.5. Elements with different salience*

The study in the literature that most closely follows the experimental design used here is a study by Gurnsey and Laundry (1992). In one of their conditions, the four quadrants contained textures of randomly oriented Ls or Xs, each of them surrounded by empty space. Both conditions were tested, i.e. search for the X texture among three L textures and search for the L texture among three X textures, and accuracy data are available. The design is basically equivalent to the one used here, but — interestingly — the asymmetries obtained in their study seem to be within the limits of the IPM (although they are also quite large). Possibly, both element types (L textures and X textures) were approximately equally salient, and had a similar 'competitive power'. A rejection of the IPM may be possible only when the two elements that are used in the asymmetric tasks have different salience, i.e. when global competition has differential effects on the two tasks.

Recently, signal-detection theory has been used to successfully account for a variety of simple search tasks such as search for a tilted line among vertical lines (Palmer et al., 1993; Palmer, 1994; Eckstein, Thomas & Whiting, 1996). Our findings suggest that simple decision models will fail as soon as asymmetric tasks with elements of different salience are tested (e.g. not only search for the bright dot among dark dots but also search for the dark dot among bright dots).

## 6. Summary

The experimental data presented here were found to be inconsistent with a simple decision model that assumes independent processing of the four quadrants followed by an ideal-observer decision. One reason for the failure may be that observers use suboptimal decision variables and that they, in addition, use different decision variables in the 1-Singleton and the 3-Singleton Tasks. Another reason for the failure of the IPM is that stimuli in the four quadrants are not — as assumed — processed independently, but that they are subject to a global competition. As for possible mechanisms of the competition one can only speculate at this point. A global response-normalization may occur; alternatively, the stimuli might compete for processing resources or memory access.

## Acknowledgements

We would like to thank Marc Repnow for developing the C library that was used in these experiments, and for his assistance in various computer-related problems; Christoph Zenger for stimulating discussions and an outline of the proof presented in Appendix A; and Steffen Egner and Oliver Landolt for their comments on an earlier version of this manuscript. Financial support was provided by the German Research Council (DFG: Forschergruppe Neuroophthalmologie and SF13 517) and by Caltech's Division of Biology.

## Appendix A. The 'optimal' ROC (Proof)

In Section 2.2, it was suggested that the ROC curves described by Sections 5 and 6 maximize and minimize performance levels in 4AFC tasks for a given performance in the 2AFC task. To prove this hypothesis[1] we assume a convex ROC $f(x)$ that is described by the corner points $P_1 = (0;0)$, $P_2$, $P_3$, …, $P_i = (x_i;y_i)$, …, $P_{n-1}$, $P_n = (1;1)$. It will be shown that any 'polygonal' ROC curve of this type can be modified (in several steps) into ROCs of the proposed forms, without reducing the performance asymmetry. The restriction to polygonal ROCs does not appear to be problematic, as any convex ROC could be approximated with infinitesimal error by a polygonal ROC. (Proof not presented.)

**Theorem 1.** *If $f$ is a measurable function, $g$ is an integrable function, and $\alpha$ and $\beta$ are real numbers such that $\alpha \le f(x) \le \beta$ almost everywhere, then there exists a real number $\gamma$, $\alpha \le \gamma \le \beta$, such that*

[1] It is my pleasure to acknowledge my father, Christoph Zenger, for providing an outline of this proof (BZ).

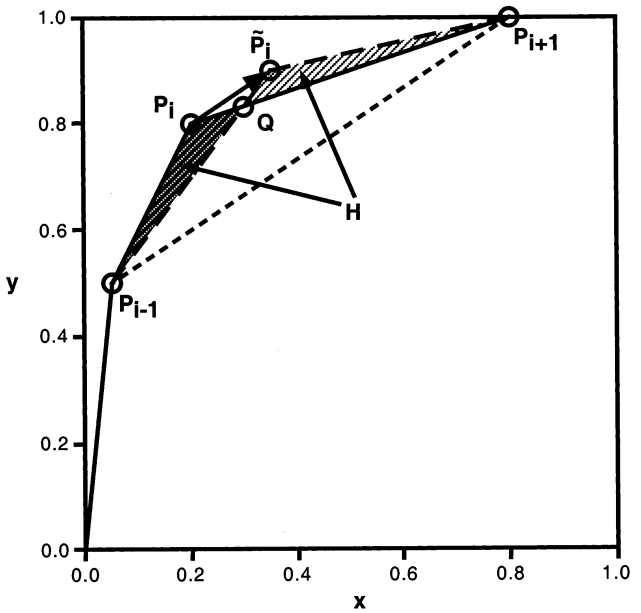


Fig. A1. The ROC is modified by shifting point $P_i$ parallel to $P_{i-1}P_{i+1}$ into positive $x$ and $y$ directions onto point $\tilde{P}_i$. This operation does not modify the area under the ROC as the two shaded areas are equivalent, and it does not reduce the performance in the 4AFC task (which is obtained by taking the ROC curve to the power of three and then integrating).

$$\int f|g|\mathrm{d}\mu = \gamma \int |g|\mathrm{d}\mu \qquad \textit{(page 114, Halmos, 1950)}.$$

Theorem 1 is known as the mean value theorem for integrals. (For a proof see standard textbooks of analysis.)

**Theorem 2.** *A convex polygonal ROC $f(x)$ with the ordinate of point $P_{i+1}$ equal to 1 can be modified to a new ROC $\tilde{f}(x)$ by shifting $P_i$ by a small amount parallel to $P_{i-1}P_{i+1}$ into positive x and y directions such that the ordinate of the new point ($\tilde{P}_i$) is less or equal to 1 (see Fig. A1). For this modification, the following holds:*

(i) $\int_0^1 \tilde{f}(x)\mathrm{d}x = \int_0^1 f(x)\mathrm{d}x$, *i.e. the area under the ROC does not change.*
(ii) $\int_0^1 \tilde{f}(x)^3\,\mathrm{d}x \geq \int_0^1 f(x)^3\,\mathrm{d}x$, *i.e. performance in the 4AFC is not reduced.*

**Proof.** (i) The areas of $\Delta P_{i-1}P_{i+1}P_i$ and $\Delta P_{i-1}P_{i+1}\tilde{P}_i$ are equivalent since the triangles have the same baseline $[P_{i-1}P_{i+1}]$ and the same height (the tip of the triangle ($P_i$) was shifted parallel to the baseline).

(ii) We write $\tilde{f}(x) = f(x) + h(x)$, with $h(x) \leq 0$ in the interval $[x_{i-1};x_Q]$ and $h(x) > 0$ in the interval] $x_Q$; $x_{i+1}$] for a specific $x_Q \in [x_{i-1};x_{i+1}]$ (see Fig. A1). The areas under $\tilde{f}$(x) and $f(x)$ are equal. Therefore we have $H := \int_{x_{i-1}}^{x_Q} |h(x)|\mathrm{d}x = \int_{x_Q}^{x_{i+1}} |h(x)|\mathrm{d}x$ with $H > 0$. For small $h(x)$, we obtain:

$$\begin{aligned}
&\int_0^1 \tilde{f}(x)^3\,\mathrm{d}x - \int_0^1 f(x)^3\,\mathrm{d}x \\
&= \int_0^1 (f(x)+h(x))^3\,\mathrm{d}x - \int_0^1 f(x)^3\,\mathrm{d}x \\
&\approx \int_0^1 f(x)^3 + 3f(x)^2h(x)\mathrm{d}x - \int_0^1 f(x)^3\,\mathrm{d}x \\
&= \int_0^1 3f(x)^2h(x)\mathrm{d}x \\
&= \int_{x_{i-1}}^{x_Q} 3f(x)^2h(x)\mathrm{d}x + \int_{x_Q}^{x_{i+1}} 3f(x)^2h(x)\mathrm{d}x \\
&= \int_{x_{i-1}}^{x_Q} -3|f(x)|^2\,|h(x)|\mathrm{d}x + \int_{x_Q}^{x_{i+1}} 3|f(x)|^2\,|h(x)|\mathrm{d}x \\
&= -3\gamma_1^2 \int_{x_{1-2}}^{x_Q} |h(x)|\mathrm{d}x + 3\gamma_2^2 \int_{x_Q}^{x_i} |h(x)|\mathrm{d}x \\
&= 3H(\gamma_2^2 - \gamma_1^2) \qquad \text{(Theorem 1)}
\end{aligned}$$

with $\gamma_1 \in [y_{i-1}; y_Q]$ and $\gamma_2 \in [y_Q; y_{i=1}]$. The ROC $f(x)$ is a monotone function. Therefore, one can see immediately that $\gamma_2^2 > \gamma_1^2$, and we can show that

$$\int_0^1 \tilde{f}(x)^3\mathrm{d}x - \int_0^1 f(x)^3\,\mathrm{d}x \geq 0.$$

**Theorem 3.** *Any convex, polygonal ROC $f(x)$ can be replaced by a polygonal ROC $f_{max}(x)$ with $P_1 = (0;0)$, $P_2 = (x_2;1)$, and $P_3 = (1;1)$, such that:*
(i) $\int_0^1 f_{\max}(x)\mathrm{d}x = \int_0^1 f(x)\mathrm{d}x$, *i.e., the area under the two ROCs is equivalent.*
(ii) $\int_0^1 f_{\max}(x)^3\,\mathrm{d}x \geq \int_0^1 f(x)^3\,\mathrm{d}x$, *i.e. performance in the 4AFC is not reduced.*

**Proof 3.** We modify $f(x)$ step by step, according to the following instruction:

Find the point with the largest index whose ordinate is less than 1. Shift this point ($P_i$) parallel to $P_{i-1}P_{i+1}$ such that the ordinate of the new point is 1. (Theorem 2 ensures that this modification does not violate the requirements i and ii.)

If one continues to follow this instruction, one obtains a ROC $f_{\max}$, of the required form (i.e. the ordinate of all $P_i$ with $i > 1$ is 1). This ROC is consistent with Eq. (5).

**Theorem 4.** *Any convex, polygonal ROC can be replaced by a ROC $f_{min}(x)$ with $P_1 = (0;0)$, $P_2 = (0;y_2)$, and $P_3 = (1;1)$, such that:*
(i) $\int_0^1 f_{\min}(x)\mathrm{d}x = \int_0^1 f(x)\mathrm{d}x$, *i.e. the area under the two ROCs is equivalent.*
(ii) $\int_0^1 f_{\min}(x)^3\mathrm{d}x \leq \int_0^1 f(x)^3\,\mathrm{d}x$, *i.e. performance in the 4AFC is not increased.*

**Proof 4.** It is easy to see that the proof can be done analogous to the proofs of Theorems 2 and 3. The only difference is that points are shifted in negative (rather than positive) $x$ and $y$ directions until the abscissa of each point is 0, and that the points are shifted in an ascending (rather than descending) index order. The resulting ROC curve $f_{\min}$ is consistent with Eq. (6).

## Appendix B. Perceptual bias

An implicit assumption in the IPM is that the activity distributions of elements A and B are the same in all four quadrants. Here, we extend the model to cases where the response distribution of elements A and B depend on the quadrant in which they are presented, i.e. we allow for perceptual bias. We denote the quadrant in which an element is presented by an index; the notation '$A_4$' indicates, e.g. that A is presented in the 4th quadrant.

The IPM assumes an ideal-observer decision which requires that the observer is able to transform the response values in each quadrant to the corresponding target-likelihood values. In the case of perceptual bias, this transformation is probably unknown to the observer at the onset of the experiment, but he or she may use the auditory feedback to determine the appropriate transformation and to recalibrate the distributions. (For example, the observer may learn that quadrant 1 always produces high responses and that a high response in this quadrant is thus not particularly indicative of target presence.) When modeling perceptual-bias effects, the assumption of an ideal observer (who is able to recalibrate the response distributions) is somewhat implausible. After all, it is exactly the point of the perceptual-bias notion that observers deviate from the ideal-observer strategy. Therefore, we assume here that observers use a maximal-or-minimal-response strategy.

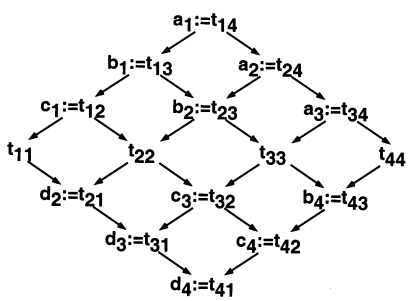


Fig. B1. Order relationship of the different $t_{ij}$, with $i,j \in \{1,2,3,4\}$. The arrows represent a '$\geq$' sign. Most of the parameters are given an alternative notation to avoid confusion with the double indexing. In tasks where element A has to be found among three elements B, the parameters are on the diagonals tilted clockwise with respect to the vertical, in tasks where element B has to be found among three elements A, the parameters are on the diagonals tilted counterclockwise with respect to the vertical.

(In cases where observers indeed recalibrate responses, one may simply look at this recalibration process as being a part of the black box.)

### *B.1. A model with 12 parameters*

#### *B.1.1. Parameterization*

Instead of the two response distributions (of elements A and B) that were relevant in the IPM, one now has to consider the response distributions of eight elements ($A_1$, $A_2$, ..., $B_4$). Rather than considering the response distributions of all eight elements, each element pair $A_iB_j$ ($i,j \in \{1, 2, 3, 4\}$) is represented by a single parameter $t_{ij}$ which corresponds to the area $R_{ij}$ under the ROC curve defined by the two elements; specifically, $t_{ij} := 2R_{ij} - 1$. The parameter $t_{ij}$ is, thus, a measure of the performance in a (hypothetical) 2AFC task where $A_i$ and $B_j$ have to be discriminated. This parameterization is analogous to the one used in the IPM ($t = 2 \cdot P_{2AF} - 1$).

#### *B.1.2. Assumptions*

To obtain constraints on the magnitude of performance asymmetries, a few assumptions need to be made. These assumptions can be viewed as extensions of those made in the IPM, with adjustments to the new situation.

- The monotonicity assumption holds for all pairs of elements $A_i$ and $B_j$ (with $i,j \in \{1, 2, 3, 4\}$), meaning that the likelihood that element $A_i$ is present rather than element $B_j$ does not decrease with increasing response.
- The order of elements along the response axis is the same for both elements, i.e. if $A_1$ produces larger responses than $A_3$, then $B_1$ produces larger responses than $B_3$. This assumption always holds, for instance, when perceptual bias consists only of additive or multiplicative constants for each quadrant. Without loss of generality we can call the element with the largest response $A_1$, the next one $A_2$ (the distributions may of course also be equal), then $A_3$, and so on, the last element being $B_4$. Of all pairs $A_iB_j$ discrimination would, thus, be best for $A_1B_4$, and worst for $A_4B_1$ ($\Rightarrow t_{14} \geq t_{41}$). The overall order relationship of the different parameters is depicted in Fig. B1.

#### *B.1.3. The role of the parameters ($t_{ij}$)*

To avoid confusion with the double indexing of the parameters, most of the $t_{ij}$ values are given an alternative notation, which is introduced in Fig. B1. Each of the possible search tasks (shown schematically in Fig. B2) is affected by three of the parameters. For instance, when $A_1$ has to be found among $B_2$, $B_3$ and $B_4$, performance is constrained by $a_1 (= t_{14})$, $b_1 (= t_{13})$, and $c_1 (t_{12})$. Note that the three parameters that correspond

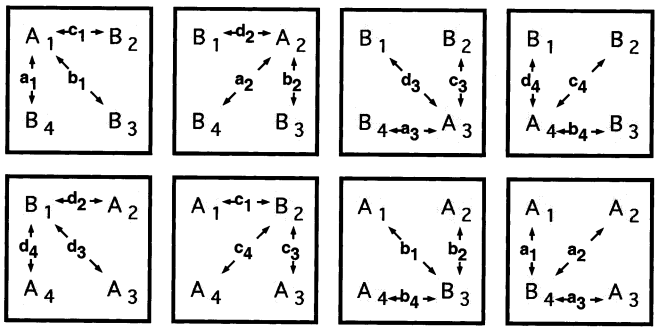


Fig. B2. Schematic diagram of all possible search tasks, demonstrating how the twelve parameters affect the different tasks.

to a specific task always fall onto a straight line in Fig. B1: in tasks where element A has to be found among three elements B, the parameters are on the diagonals tilted clockwise with respect to the vertical, in tasks where element B has to be found among three elements A, the parameters are on the diagonals tilted counterclockwise with respect to the vertical.

*B.1.4. Maximizing the performance asymmetry*

Assume a specific task is constrained by the parameters $t_1$, $t_2$, and $t_3$ — what are the upper bound ($P_\uparrow$) and the lower bound ($P_\downarrow$) of the performance? In the IPM (when $t_1 = t_2 = t_3 =: t$) maximal and minimal performance are described by Eqs. (8) and (7). These equations can easily be generalized for the bias situation and one obtains:

$$P_\uparrow(t_1,t_2,t_3) = \int_0^1 f(x,t_1)f(x,t_2)f(x,t_3)\mathrm{d}x = \frac{1+t_3}{2} - \frac{(1-t_1)^3}{12(1-t_2)(1-t_3)} - \frac{(1-t_2)^2}{6(1-t_3)} \quad \text{(B1)}$$

$$P_\downarrow(t_1,t_2,t_3) = \int_0^1 g(x,t_1)g(x,t_2)g(x,t_3)\mathrm{d}x = \frac{t_1t_2t_3}{4} + \frac{(t_1t_2+t_1t_3+t_2t_3)}{12} - \frac{(t_1+t_2+t_3)^2}{12} + \frac{1}{4} \quad \text{(B2)}$$

In cases where denominators in Eq. (B1) are zero ($t_2 = t_1 = 1$, and $t_3 = t_2 = t_1 = 1$), the problematic terms can be canceled out of the fraction. These special cases do, thus, not provide additional problems and are not considered separately in the following analysis.

The performance when searching for element A cannot be better than $P_{\max}$:

$$P_{\max} = \frac{1}{4}[P_\uparrow(a_1,b_1,c_1) + P_\uparrow(a_2,b_2,d_2) + P_\uparrow(a_3,c_3,d_3) + P_\uparrow(b_4,c_4,d_4)] \quad \text{(B3)}$$

and the performance when searching for element B cannot be below $P_{\min}$:

$$P_{\min} = \frac{1}{4}[P_\downarrow(a_1,a_2,a_3) + P_\downarrow(b_1,b_2,b_4) + P_\downarrow(c_1,c_3,c_4) + P_\downarrow(d_2,d_3,d_4)] \quad \text{(B4)}$$

It is possible to analytically derive the parameter choice that maximizes performance asymmetries. We will do this by first showing that if one is interested only in an upper limit for performance asymmetries, the number of parameters can be reduced. Before starting with the parameter reduction, we consider what happens to $P_\downarrow(t_1, t_2, t_3)$ when one of the parameters is modified.

*B.2. Changing a parameter in $P_\downarrow(t_1,t_2,t_3)$*

Differentiating Eq. (B2) with respect to $t_1$, we obtain

$$\frac{\mathrm{d}P_\downarrow(t_1,t_2,t_3)}{\mathrm{d}t_1} = \frac{1}{4}t_2t_3 + \frac{1}{12}(t_2+t_3) + \frac{1}{12}. \quad \text{(B5)}$$

To simplify the notation one can define

$$D(x_1,x_2) := \frac{1}{4}x_1x_2 + \frac{1}{12}(x_1+x_2) + \frac{1}{12} \quad \text{(B6)}$$

and can rewrite Eq. (B5) as

$$\frac{\mathrm{d}P_\downarrow(t_1,t_2,t_3)}{\mathrm{d}t_1} = D(t_2,t_3). \quad \text{(B7)}$$

For the other two derivatives we consequently obtain:

$$\frac{\mathrm{d}P_\downarrow(t_1,t_2,t_3)}{\mathrm{d}t_2} = D(t_1,t_3) \quad \text{(B8)}$$

$$\frac{\mathrm{d}P_\downarrow(t_1,t_2,t_3)}{\mathrm{d}t_3} = D(t_1,t_2) \quad \text{(B9)}$$

It is easy to see that

$$t_1 \geq t_3 \quad \text{and} \quad t_2 \geq t_4 \Rightarrow D(t_1,t_2) \geq D(t_3,t_4), \quad \text{(B10)}$$

an implication that will be used below.

*B.3. Parameter reduction*

*B.3.1. Step 1: reduction from 12 → 8*

In a first step, the larger two of the three parameters that affect search for item $A_i$ are replaced by their mean ($m_i$). These operations are illustrated in Fig. B3. As we will show here, this does neither decrease $P_{\max}$, nor increase $P_{\min}$ (i.e. the asymmetry does not decrease). Writing $t_1 = m + x$ and $t_2 = m - x$ (with $m = (t_1 + t_2)/2$ and $x > 0$) and differentiating with respect to $x$ one obtains:

$$\frac{\mathrm{d}P_\uparrow(m+x,m-x,t_3)}{\mathrm{d}x} = \frac{1}{3(1-t_3)(1-m+x)^2} \times \underbrace{((1-m-x)^2(1-m+x/2) - (1-m+x)^3)}_{\leq 0} \leq 0 \quad \text{(B11)}$$

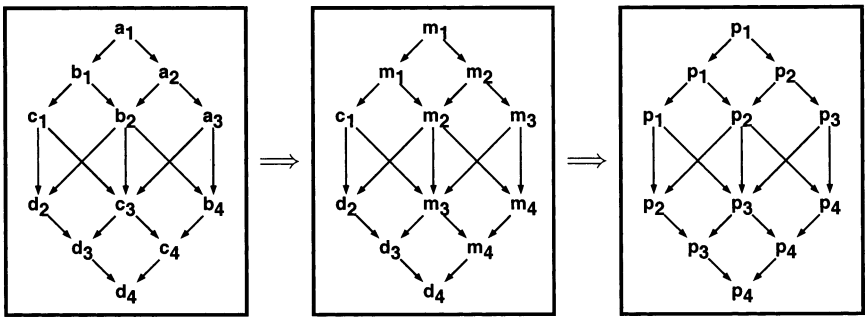


Fig. B3. Summary of the first and second step of parameter reduction. First, the larger two parameters in search for item $A_i$ are replaced by their mean ($m_i$), then all three parameters in search for $A_i$ are replaced by their mean.

When $x$ is reduced (until $x=0$), $P_\uparrow$ increases, or does, at least, not decrease. In other words, if the first two parameters of $P_\uparrow$ are replaced by their mean, $P_\uparrow$ does not decrease (i.e. $\Delta P_\uparrow \geq 0$). One can also show that $P_{\min}$ does not increase: for instance, if we first replace $a_1$ and $b_1$ by their mean ($m_1$), we find that $\Delta P_{\min} \leq 0$ because $-D(a_2,a_3)+D(b_2,b4) \leq 0$ (see Eq. (B10)). Similarly, one can show that replacing $a_2$ and $b_2$ by their mean ($m_2$), $a_3$ and $c_3$ by their mean ($m_3$), and $b_4$ and $c_4$ by their mean ($m_4$) does not decrease the performance asymmetry either. After step 1, the number of parameters has been reduced from 12 to 8.

### B.4. Step 2: reduction from 8 → 4

In the next step, the three parameters in $P_\uparrow(m, m, t)$ are replaced by their mean ($p=(2m+t)/3$), reducing the number of parameters from 8 to 4 (see Fig. B3). Like in the previous step, one can show that this does not lead to a reduction of $P_\uparrow$ by showing that $\mathrm{d}P_\uparrow(p+x, p+x, p-2x)/\mathrm{d}x \leq 0$ (for $x \geq 0$):

$$\frac{\mathrm{d}P_\uparrow(p+x,p+x,p-2x)}{\mathrm{d}x} = -1+\frac{1}{2}\underbrace{\frac{(1-p-x)}{(1-p+2x)}}_{\leq 1}+\frac{1}{2}\underbrace{\frac{(1-p-x)^2}{(1-p+2x)^2}}_{\leq 1} \leq 0 \quad \text{(B12)}$$

Again, $P_{\min}$ does not decrease. If we replace $m_1$ and $c_1$ by $p_1 := (2m_1+c_1)/3$, for example, we find that $\Delta P_{\min} \leq 0$, because of $-D(m_2,m_3)-D(m_2,m_4)+2D(m_3,m_4) \leq 0$ (see Eq. (B10)). The same holds for replacing $m_2$ and $d_2$ by $p_2 := (2m_2+d_2)/3$, $m_3$ and $d_3$ by $p_3 := (2m_3+d_3)/3$, and $m_4$ and $d_4$ by $p_4 := (2m_4+d_4)/3$.

#### B.4.1. Step 3: reduction from 4 → 1

The four-parameter version of the bias model can be obtained by inserting the new parameters into Eqs. (B3) and (B4). One obtains for $P_{\max}$ and $P_{\min}$:[2]

$$P_{\max} = \frac{3}{16}(p_1+p_2+p_3+p_4)+\frac{1}{4} \quad \text{(B13)}$$

$$P_{\min} = \frac{1}{16}(p_1p_2p_3+p_1p_2p_4+p_1p_3p_4+p_2p_3p_4) + \frac{1}{24}(p_1p_2+p_1p_3+p_1p_4+p_2p_3+p_2p_4+p_3p_4) + \frac{1}{16}(p_1+p_2+p_3+p_4)+\frac{1}{4} \quad \text{(B14)}$$

What choice of parameters $p_1$, $p_2$, $p_3$ and $p_4$ will maximize the asymmetry? As $P_{\max}$ only depends on the mean of these four parameters, one can restate the question as follows: for a given mean value of the parameters, how can performance in the difficult task (search for element B) be minimized? What happens, e.g. when parameter $p_1$ is increased and parameter $p_2$ is decreased? Writing $p_1 = m+x$ and $p_2 = m-x$, and using Eq. (B14) we obtain

$$\frac{\mathrm{d}P_{\min}}{\mathrm{d}x} = -2x\left(\frac{1}{16}p_3+\frac{1}{16}p_4+\frac{1}{24}\right) \quad \text{(B15)}$$

Assuming $p_1 \geq p_2$ implies $x \geq 0$ and we thus obtain a non-positive derivative, meaning that increasing $x$ does not increase $P_{\min}$. Since $P_{\max}$ is not affected by the operation, the performance asymmetry increases (or does, at least, not decrease). Eq. (B14) is symmetric with respect to the four parameters $p_1$, $p_2$, $p_3$ and $p_4$. Therefore, if there are at least two parameters $p_\alpha$ and $p_\beta$ such that $0 < p_\alpha \leq p_\beta < 1$, the performance asymmetry can be increased (or at least, will not be reduced) by increasing $p_\beta$ and reducing $p_\alpha$. From this follows that, in the optimal solution, at least three of the four parameters have to be equal to either 0 or 1. Taken together, four different solutions are possible for the four p parameters: (1,1,1,$p$), (1,1,$p$,0), (1,$p$,0,0), and ($p$,0,0,0).

### B.5. Bias-model predictions

The model predictions for the upper limit of performance asymmetries can be obtained by inserting each

[2] Interestingly, these equations are equivalent to the predictions that a highthreshold model would make when diferent detection probabilities $p_1$, $p_2$, $p_3$, and $p_4$ are assumed for the salient element (here element A) in the different quadrants.

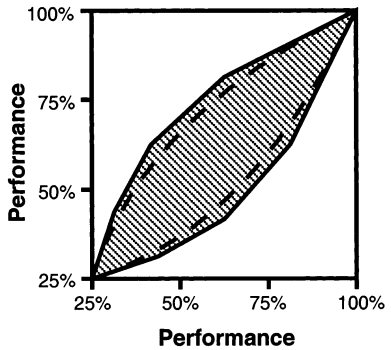


Fig. B4. Maximal performance asymmetries predicted by the IPM (dashed lines) and the bias model (solid lines).

of these four solutions into Eqs. (B13) and (B14). After eliminating $p$ one obtains for a given performance in the easy task ($P_{\max}$ a lower limit $P_{\min}$ for the difficult task.

$$P_{\min}\begin{cases} 2(P_{\max}-\frac{1}{2}) & 1 \geq P_{\max} \geq \frac{13}{16} \\ \frac{10}{9}(P_{\max}-\frac{1}{4}) & 1 \geq P_{\max} \geq \frac{10}{16} \\ \frac{5}{9}(P_{\max}+\frac{1}{8}) & 1 \geq P_{\max} \geq \frac{7}{16} \\ \frac{1}{3}(P_{\max}+\frac{1}{2}) & 1 \geq P_{\max} \geq \frac{1}{4} \end{cases} \quad \text{(B16)}$$

This limit consists of four linear sections; it is presented together with the limit of the IPM in Fig. B4. As one can see, the limit is not much increased, in spite of the fact that the assumptions of the IPM have been relaxed dramatically.

Note that the model allows for rather extreme situations: there may, e.g. be a case where in two quadrants the salient element is always detected while it is never detected in the other two quadrants. In spite of the generality of the model assumptions, we show here that it is possible to derive narrow constraints on the magnitude of performance asymmetries. These constraints are inconsistent with psychophysical data, implying that the perceptual-bias effects considered here cannot account for the failure of the IPM.

## References


Ahissar, M., & Hochstein, S. (1993). Attentional control of early perceptual learning. *Proceedings of the National Academy of Sciences USA*, *90*, 5718–5722.

Ahissar, M., & Hochstein, S. (1996). Learning pop-out detection: specificities to stimulus characteristics. *Vision Research*, *36*, 3487–3500.

Atkinson, J., & Braddick, O. (1989). 'Where' and 'what' in visual search. *Perception*, *18*, 181–189.

Bach, M. (1991). Stufenlos. Anti-aliasing von Mac-Grafiken unter Quickdraw. *Computertechnik*, *12*, 260–262.

Bacon, W., & Egeth, H. (1991). Local processes in preattentive feature detection. *Journal of Experimental Psychology*: *Human Perception and Performance*, *17*, 77–90.

Bergen, J., & Julesz, B. (1983). Parallel versus serial processing in rapid pattern discrimination. *Nature*, *303*, 696–698.

Braun, J. (1994). Visual search among items of different salience: removal of visual attention mimics a lesion in extrastriate area V4. *The Journal of Neuroscience*, *14*, 554–567.

Braun, J. (1998). Divided attention: narrowing the gap between brain and behavior. In R. Parasuraman, *The attentive brain*. Cambridge, MA: MIT Press (in press).

Braun, J., & Julesz, B. (1998). Withdrawing attention at little or no cost: detection and discrimination tasks. *Perception & Psychophysics*, *60*(1), 1–23.

Braun, J., & Sagi, D. (1990). Vision outside the focus of attention. *Perception and Psychophysics*, *48*, 45–58.

Broadbent, D. (1958). *Percpetion and communication*. London: Pergamon.

Cohen, A. (1993). Asymmetries in visual search for conjunctive targets. *Journal of Experimental Psychology*: *Human Perception and Performance*, *19*, 775–797.

Desimone, R., & Duncan, J. (1995). Neural mechanisms of selective visual attention. *Annual Reviews of Neuroscience*, *18*, 193–222.

Driver, J., & McLeod, P. (1992). Reversing visual search asymmetries with conjunctions of movement and orientation. *Journal of Experimental Psychology*: *Human Perception and Performance*, *18*, 22–33.

Duncan, J., & Humphreys, G. (1989). Visual search and stimulus similarity. *Psychological Review*, *96*, 433–458.

Duncan, J., & Humphreys, G. (1992). Beyond the search surface: visual search and attentional engagement. *Journal of Experimental Psychology*: *Human Perception and Performance*, *18*, 578–588.

Eckstein, M. (1998). The lower visual search efficiency for conjunctions is due to noise and not serial attentional processing. *Psychological Science*, *9*(2), 111–118.

Eckstein, M., Thomas, J., & Whiting, J. (1996). Predicting visual search accuracy in symbolic displays and medical images. *Perception* (*Supplement*), *25*, 5.

Eckstein, M., & Whiting, J. (1996). Visual signal detection in structured backgrounds i. effect of number of possible spatial locations and signal contrast. *Journal of the Optical Society of America*, *A*, *13*(9), 1777–1787.

Foley, J., & Schwarz, W. (1998). spatial attention: effect of position uncertainty and number of distractor patterns on the threshold-versus-contrast function for contrast discrimination. *Journal of the Optical Society of America*, *A*, *15*(5), 1036–1047.

Green, D., & Swets, J. (1966). *Signal detection theory and psychophysics*. Huntington, New York: Krieger.

Gurnsey, R., & Browse, R. (1987). Micropattern properties and presentation conditions influencing visual texture discrimination. *Perception Psychophysics*, *41*, 239–252.

Gurnsey, R., & Browse, R. (1989). Asymmetries in visual texture discrimination. *Spatial Vision*, *4*, 31–44.

Gurnsey, R., & Laundry, D. (1992). Texture discrimination with and without abrupt texture gradients. *Canadian Journal of Psychology*, *46*, 306–332.

Halmos, P. (1950). *Measure theory*. *The university series in higher mathematics*. Van Nostrand.

Karni, A., & Sagi, D. (1991). Where practice makes perfect in texture discrimination: evidence for primary visual cortex plasticity. *Proceedings of the National Academy of Sciences USA*, *88*, 4966–4970.

Laarni, I, Nasanen, R., Rovamo, J., & Saarinen, J. (1996). Performance in simple visual search at threshold. *Investigative Ophthalmology and Visual Science*, *37*, 1706–1710.

Lee, D., Koch, C., & Braun, J. (1997). Spatial vision thresholds in the near absence of attention. *Vision Research*, *37*, 2409–2418.

Luck, S., & Vogel, E. (1997). The capacity of visual working memory for features and conjunctions. *Nature*, *390*, 279–281.

Meigen, T., Lagreze, W., & Bach, M. (1994). Asymmetries in preattentive line detection. *Vision Research*, *34*, 3103–3109.

Miller, G. (1956). The magical number seven, plus or minus two. *Psychological Review*, *63*, 81–97.

Müller, H., & Humphreys, G. (1991). Luminance-increment detection: capacity-limited or not? *Journal of Experimental Psychology*: *Human Perception and Performance*, *17*, 107–124.

Nagy, A., & Cone, S. (1996). Asymmetries in simple feature searches for color. *Vision Research*, *36*, 2837–2847.

Nothdurft, H. (1985). Sensitivity for structure gradient in texture discrimination tasks. *Vision Research*, *25*, 1957–1968.

Nothdurft, H. (1991). Texture segmentation and pop-out from orientation contrast. *Vision Research*, *31*, 1073–1078.

Palmer, J. (1994). Set-size effects in visual search: the effect of attention is independent of the stimulus for simple tasks. *Vision Research*, *34*, 1703–1721.

Palmer, I., Ames, T., & Lindsey, D. (1993). Measuring the effect of attention on simple visual search. *Journal of Experimental Psychology*: *Human Perception and Performance*, *19*, 108–130.

Palmer, I., Verghese, P., & Pavel, P. (2000). The psychophysics of visual search. *Vision Research*, *40*, 1227–1268.

Pelli, D. (1985). Uncertainty explains many aspects of visual contrast detection and discrimination. *Journal of the Optical Society of America*, *A*, *2*, 1508–1532.

Posner, M. (1980). Orienting of attention. *Quarterly Journal of Experimental Psychology*, *32*, 3–25.

Rubenstein, B., & Sagi, D. (1990). Spatial variability as a limiting factor in texture-discrimination tasks: implications for performance asymmetries. *Journal of the Optical Society of America*, *A*, *7*, 1632–1643.

Sagi, D., & Julesz, B. (1985). 'Where' and 'what' in vision. *Science*, *228*, 1217–1219.

Schneider, W., & Shiffrin, R. (1977). Controlled and automatic human information processing: I. Detection, search, and attention. *Psychological Review*, *84*, 1–66.

Solomon, I., Lavie, N., & Morgan, M. (1997). Contrast discrimination function: spatial cuing effects. *Journal of the Optical Society of America*, *A*, *14*, 2443–2448.

Treisman, A., & Gelade, G. (1980). A feature-integration theory of attention. *Cognitive Psychology*, *12*, 97–136.

Treisman, A., & Gormican, S. (1988). Feature analysis in early vision: evidence from search asymmetries. *Psychological Review*, *95*, 15–48.

Treisman, A., & Souther, J. (1985). Search asymmetry: a diagnostic for preattentive processing of separable features. *Journal of Experimental Psychology*: *General*, *114*, 285–310.

Trick, L., & Pylyshyn, Z. (1994). Why are small and large numbers enumerated differently? A limited-capacity preattentive stage in vision. *Psychological Review*, *101*, 80–102.

Verghese, P., & Nakayama, K. (1994). Stimulus discriminability in visual search. *Vision Research*, *34*, 2453–2467.

Wolfe, J. (1994). Guided search 2.0: a revised model of visual search. *Psychonomic Bulletin & Review*, *1*, 202–238.

Zenger, B., & Fahle, M. (1997). Missed targets are more frequent than false alarms: a model for error rates in visual search. *Journal of Experimental Psychology*: *Human Perception and Performance*, *23*, 1783–1791.